Separation Science and Technology
Publication details, including instructions for authors and subscription information:
http://www.informaworld.com/smpp/title~content=t713708471

Role of Bubble Size in Flotation of Coarse and Fine Particles—A Review

D. Tao[a]
[a] Department of Mining Engineering, University of Kentucky, Lexington, Kentucky, USA

Online publication date: 08 July 2010

To cite this Article Tao, D.(2005) 'Role of Bubble Size in Flotation of Coarse and Fine Particles—A Review', Separation Science and Technology, 39: 4, 741 — 760
To link to this Article: DOI: 10.1081/SS-120028444
URL: http://dx.doi.org/10.1081/SS-120028444

SEPARATION SCIENCE AND TECHNOLOGY
Vol. 39, No. 4, pp. 741–760, 2004

Role of Bubble Size in Flotation of Coarse and Fine Particles—A Review

D. Tao*

Department of Mining Engineering, University of Kentucky, Lexington, Kentucky, USA

ABSTRACT

Froth flotation is the dominating mineral beneficiation technique and has achieved great commercial success. This process has also found many applications in other industries where physical separation of materials is needed. However, its high process efficiency is often limited to a narrow particle size range of approximately 10–100 μm. Considerable efforts have been made to extend this size range to the lower limit of a few microns, even submicrons, and the upper limit of 1–2 mm, in response to increased needs for higher process efficiency and expanded applications of flotation. The particle–bubble collision, attachment, and detachment are the most critical steps in the flotation process. These individual elementary processes (microprocesses) and their effects on

*Correspondence: D. Tao, Department of Mining Engineering, University of Kentucky, 234E MMRB, Lexington, KY 40506-0107, USA; Fax: (859) 323-1962; E-mail: dtao@engr.uky.edu.

DOI: 10.1081/SS-120028444 0149-6395 (Print); 1520-5754 (Online)

flotation efficiency are discussed and the most recent findings are reviewed. The low flotation recovery of fine particles is mainly due to the low probability of bubble–particle collision, while the main reason for poor flotation recovery of coarse particles is the high probability of detachment of particles from the bubble surface. Fundamental analysis indicated that use of smaller bubbles is the most effective approach to increase the probability of collision and reduce the probability of detachment.

Key Words: Attachment; Coarse particle; Collision; Detachment; Flotation; Picobubble; Fine particle; Hydrodynamic cavitation.

INTRODUCTION

Froth flotation is the most widely used physical separation process for minerals processing. The vast majority of minerals are beneficiated by flotation due to its high separation efficiency and cost effectiveness. In this process hydrophobic particles captured by air bubbles ascend to the top of the pulp zone and eventually report to the froth product, whereas hydrophilic particles remain in the pulp and are discharged as tailings. However, its high process efficiency is limited to a very narrow particle size range, which is usually 10–100 μm.[1–5] The low flotation efficiency of fine particles is mainly due to the low probability of bubble–particle collision, while the main reason for poor flotation recovery of coarse particles is the high probability of detachment of particles from the bubble surface.[6–10] Since most ores require fine grinding for liberation that results in the production of large quantities of micron or submicron fine particles, most of the earlier studies on the effect of particle size on flotation have been focused on fine or ultrafine particles. In contrast, the flotation behavior of coarse particles was essentially overlooked until very recently.[8,11–17]

FLOTATION FUNDAMENTALS

The key to the success of effective particle separation by flotation is the efficient capture of hydrophobic particles by air bubbles, which is accomplished in three distinct processes: collision, adhesion, and detachment, as shown in Fig. 1. To understand the effect of particle size on flotation, particularly the floatability of fine and coarse particles, each of the successive steps has to be well understood.

MARCEL DEKKER, INC.
270 Madison Avenue, New York, New York 10016

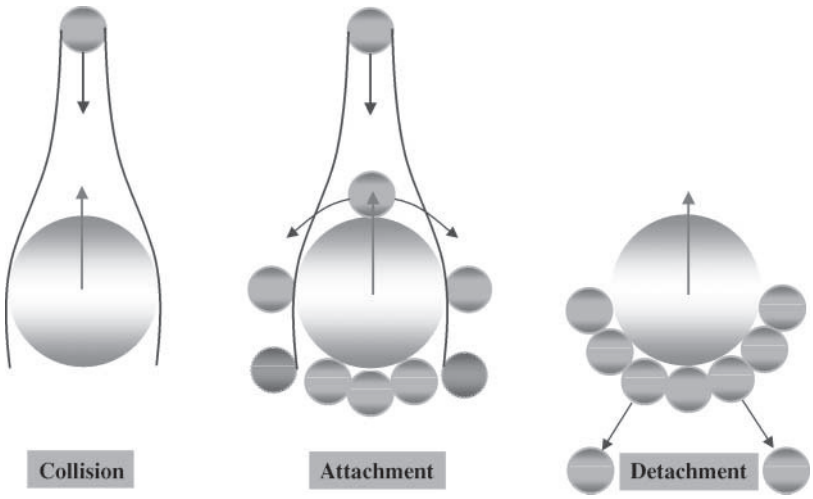

Figure 1. Illustration of three microprocesses in flotation.

Particle–Bubble Collision

The first step involved in flotation is the process of particle–bubble collision during which a particle collides with a bubble as a result of a sufficiently close encounter. This process is primarily determined by hydrodynamics of the flotation environment. The probability of collision (P_c) can be calculated from stream functions for quiescent conditions[18–20] and microturbulence models for well-mixed conditions.[10,21]

The first model of bubble–particle collision was proposed by Sutherland[22] for the condition of potential flow:

$$P_c = \frac{3D_p}{D_b} \tag{1}$$

where D_b is the bubble size and D_p the particle size. This model is valid only when bubbles are very large and water in a flotation cell is nonviscous, neither of which is realistic. As a result, it cannot be used to accurately describe the flotation process.

Gaudin[23] developed a model for very small bubbles under the Stoke's flow condition:

$$P_c = \frac{3}{2}\left(\frac{D_p}{D_b}\right)^2 \tag{2}$$

Marcel Dekker, Inc.
270 Madison Avenue, New York, New York 10016

using the stream function for the Stokes flow. Equation (2) is quite accurate when bubble size is smaller than approximately 100 μm, above which Gaudin's model significantly underestimates the collision probability.

Neither Sutherland's nor Gaudin's model can be applied to flotation processes that take place using intermediate bubble sizes not covered by Eqs. (1) and (2). For the intermediate range of Reynolds numbers of bubbles, Weber and Paddock[18,19] developed the following expression using analytical and numerical methods:

$$P_c = \frac{3}{2}\left[1 + \frac{(3/16)Re^{0.72}}{1 + 0.249Re^{0.56}}\right]\left(\frac{D_p}{D_b}\right)^2 \tag{3}$$

where Re is Reynolds number.

Using a dimensionless stream function, Yoon and Luttrell[20] derived an equation for P_c,

$$P_c = \left[\frac{3}{2} + \frac{4Re^{0.72}}{15}\right]\left(\frac{D_p}{D_b}\right)^2 \tag{4}$$

which is similar to Eq. (3) with slightly different coefficient. In fact, Yoon and Luttrell[20] showed experimentally that both Eqs. (3) and (4) gave accurate prediction of P_c as a function of D_b. An important conclusion derived from Eqs. (3) and (4) is that P_c increases with the square of the ratio of particle size to bubble size; it also depends on the bubble Reynolds number.

The aforementioned models are all based on the interceptional collision model that neglects particle inertial forces. A more comprehensive collision model was proposed by Schulze[24] who considers that the overall collision probability is the sum of three different effects, i.e., interceptional (P_c^{ic}), gravitational (P_c^{g}), and inertial (P_c^{in}). Schulze[24] suggested that the interceptional and gravitational collision probabilities be determined using the Weber–Paddock collision model and the inertial probability, (P_c^{in}), using the Plate model:[24,25]

$$P_c^{in} = \left(\frac{1}{1 + v_p/v_b}\right)\left(\frac{K}{K + a}\right)^b (1 + D_p/D_b)^2 \tag{5}$$

where K is the Stokes number, v_b is the rising velocity of the bubble, v_p is the settling velocity of the particle, and the constants a and b are Reynolds number-dependent coefficients whose values are shown in Table 1.

The influence of inertial forces on collision efficiency depends on the Stokes number K. If K is substantially larger than the critical value (K_{cr}) for a particle to reach the surface of a bubble, inertial deposition of particles onto

Marcel Dekker, Inc.
270 Madison Avenue, New York, New York 10016

Table 1. Values of a and b.[24]

Re	>500	250–500	100–250	50–100	25–50	5–25	<25
a	0.5	0.6	0.8	1.12	2.06	2.48	1.3
b	2	2	2	1.84	2.06	1.95	3.7

the bubble surface is the main collision mechanism and the collision process can be described mainly by the Langmuir–Blodgett model:[26,27]

$$P_c = \left(\frac{K}{K+0.2}\right)^2 \tag{6}$$

when $K \ll K_{cr}$, the interception is the main collision mechanism and Eq. (3) or (4) applies. However, the flotation conditions in most industrial flotation cells are in the intermediate range of the Stokes number and, therefore, both the interceptional and the inertial collision probabilities should be considered. A more detailed discussion of significance of inertial forces in collision can be found elsewhere.[9]

All particle–bubble collision models described previously show that P_c increases with increasing particle size and decreasing bubble size. Fine particles have low probability of collision with bubbles and are thus difficult to catch by bubbles, particularly by large bubbles. This is the main reason for the low flotation rate of fine particles.

There are a number of other models that describe particle–bubble collision in flotation. They include the Flint–Howarth model, the Anfruns–Kitchener model, the Nguyen–Van model, the Dukhin or GSE model, etc. A thorough review of these models is provided by Dai et al.[28]

Particle Attachment to Bubble

If a particle is sufficiently hydrophobic, the liquid film between the bubble and the particle thins and ultimately ruptures as a result of the attractive surface forces. This is followed by the establishment of the three-phase line of contact. Only those hydrophobic particles whose induction time is smaller than the sliding time can be attached to air bubbles. Obviously the attachment process is selective and the difference in attachment probability (P_a) of different particles determines the selectivity of flotation. The attachment process is determined by hydrodynamic and surface forces of particles and bubbles. Yoon[10] has shown that the probability of adhesion can be determined from the induction times or predicted using various surface

chemistry parameters that determine the surface forces of particles and bubbles.

Luttrell and Yoon[29] and Mao and Yoon[30] suggested that P_a is related to the energy barrier for the bubble–particle adhesion E_1 and the kinetic energy of collision E_k in Eq. (7):

$$P_a = \exp\left(-\frac{E_1}{E_k}\right) \tag{7}$$

It has been found[10,20,29] that P_a can be calculated using Eq. (8):

$$P_a = \sin^2\left[2\tan^{-1}\exp\left(-\frac{45 + 8Re^{0.72}u_b t_i}{15D_b(D_b/D_p + 1)}\right)\right] \tag{8}$$

where t_i is the induction time and u_b is the bubble rise velocity. Equation (8) was obtained under the presumption that particle–bubble collision occurs uniformly over the entire upper half of the bubble surface, which may not be correct.[25] Ralston et al.[31,32] derived a more general equation for calculating P_a:

$$P_a = \frac{\sin^2\left[2\tan^{-1}\exp\left(-[(2(u_p + u_b) + (u_p + u_b)(D_b/(D_b + D_p))^3/(D_b + D_p)]t_i\right)\right]}{2\beta((1+\beta^2)^{1/2} - \beta)} \tag{9}$$

where

$$\beta = \frac{12D_b}{D_p}\frac{\rho_f}{\rho_p - \rho_f}\frac{1}{Re} \tag{10}$$

in which ρ_f and ρ_p are fluid and particle densities, respectively. It should be pointed out that neither Eq. (8) nor Eq. (9) is accurate for predicting the attachment probability of coarse particles where bubble surface deformation and consequent particle rebound are significant. Nevertheless, both Eqs. (8) and (9) indicate that P_a decreases with increasing D_p, suggesting that coarse particles are more difficult to attach to air bubbles.

Dai et al.[25] and Ralston et al.[31,32] studied the effect of particle size on attachment efficiency both experimentally and analytically. They found that P_a decreases with increasing particle size and increases with increasing particle hydrophobicity. Yoon and Luttrell[20] showed that P_a increases with decreasing induction time and decreasing particle size; P_a also increases with decreasing bubble size until the bubble size becomes too small. These conclusions are in agreement with Eqs. (8) and (9). Although use of higher dosage of collector improves particle hydrophobicity and thus increases P_a,

Marcel Dekker, Inc.
270 Madison Avenue, New York, New York 10016

it increases flotation operating cost. A better approach to increase P_a may be the use of smaller bubbles.

Particle Detachment from Bubble

All particles attached to air bubbles do not report to the froth phase. Some of them detach from the bubble surface and drop back into the pulp phase. Particle detachment occurs when detachment forces exceed the maximum adhesive forces. One potential source of excessive forces is bubble oscillations caused by particle–bubble collisions. Kirchberg and Topfer[33] showed that bubble collisions with large particles resulted in detachment of many particles from the bubble surface. Cheng and Holtham[34] measured particle–bubble detachment forces by means of a vibration technique and found that the amplitude of oscillations imposed on the bubble is the dominant factor in the detachment process.

There are many forces acting between a bubble and an attached particle.[7,31,32] They are usually classified into four categories: the capillary force F_p; excess force F_e, which is the difference between the excess pressure in the bubble (favoring attachment) and the hydrostatic force (favoring detachment); real weight of particle in the liquid medium F_w; and other forces such as the hydrodynamic drag force F_d. These forces are typically represented by the following equations:

$$F_p = \frac{\pi D_p \gamma (1 - \cos\theta_d)}{2} \tag{11}$$

$$F_e = \frac{1}{4}\pi D_p^2 (1 - \cos\theta_d)\left(\frac{2\gamma}{D_b} - \frac{\rho_w g D_b}{2}\right) \tag{12}$$

$$F_w = \frac{1}{6}\pi D_p^3 \rho_p g - \frac{1}{8}\pi D_p^3 \rho_w g\left[\frac{2}{3} + \cos\left(\frac{\theta_d}{2}\right) - \left(\frac{1}{3}\right)\cos^3\left(\frac{\theta_d}{2}\right)\right] \tag{13}$$

$$F_d = 3\pi D_p \eta u \tag{14}$$

where γ is the liquid surface tension; ρ_p and ρ_w the densities of the particle and water, respectively; η is the dynamic viscosity of fluid, u is the particle rising velocity, and θ_d is the critical value of three-phase contact angle right before detachment. Of these four categories of forces, F_p is generally considered to be the major adhesion force; F_w and F_d are always the detachment force. However, the role of F_e depends on the relative magnitude of the excess pressure in the bubble and the hydrostatic force. When $2\gamma/D_b > \rho_w g D_b/2$ or $D_b < 5.5$ mm, the excess force works against detachment. Under normal flotation conditions, $D_b < 5.5$ mm. Therefore, F_e should be considered as the attachment force.

Assuming $D_b = 1\,\text{mm}$, $\theta_d = 90^\circ$, $\gamma = 72.94\,\text{dyn/cm}$, $\rho_p = 2.5\,\text{g/cm}^3$, $\rho_w = 1.0\,\text{g/cm}^3$, $g = 980\,\text{cm/s}^2$, $\eta = 0.01\,\text{dyn sec/cm}^2$, and $u = 10\,\text{cm/sec}$, one can determine the magnitude of these forces as a function of D_p. The results are shown in Fig. 2.

At the moment of detachment, the sum of the capillary force and the excess force is at equilibrium with the sum of the weight and the drag force:

$$(F_p + F_e) - (F_w + F_d) = 0 \tag{15}$$

Since F_d is negligible compared to F_w, as shown in Fig. 2, Eq. (15) can be simplified to:

$$(F_p + F_e) - F_w = 0 \tag{16}$$

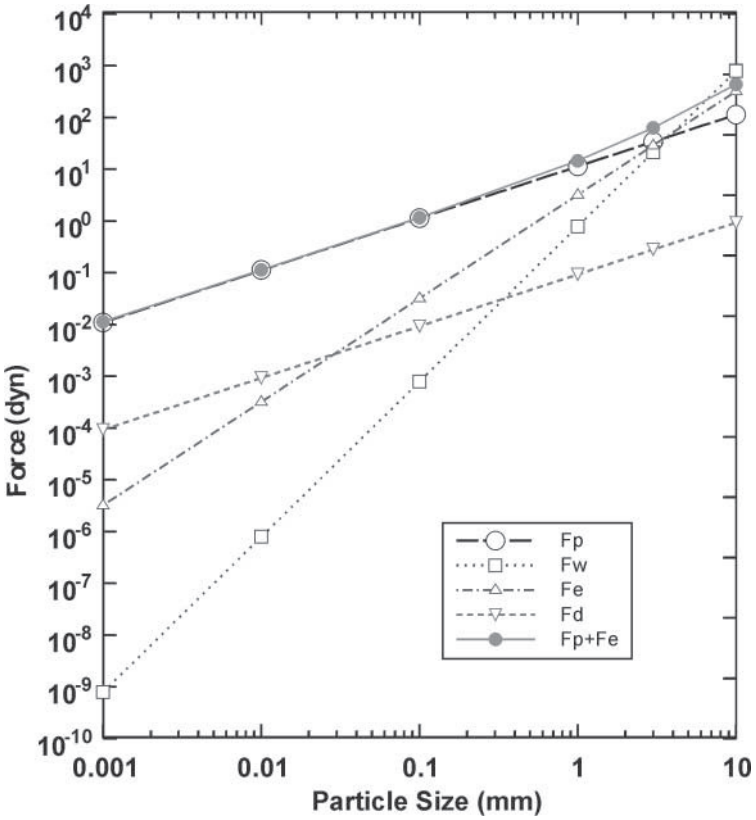

Figure 2. Magnitude of different forces as a function of particle size.

Figure 2 indicates that the attachment force is dominated by the capillary force when the particle size is smaller than about 1 mm; the excess force approaches the capillary force with increasing particle size and exceeds the capillary force at about 5 mm. For the hypothetical conditions mentioned earlier, the detachment occurs to particles larger than about 7 mm, which can be considered as the upper size limit of flotation.

It is very interesting to point out that the excess force increases with decreasing bubble size D_b, which means that smaller bubbles can be used to reduce coarse particle detachment and increase the upper flotation limit. This finding is significant, since it proves from the viewpoint of flotation fundamentals that flotation recovery of coarse particles can be enhanced using smaller rather than larger bubbles.

Under turbulent conditions, the upper size limit in flotation is reached when the dynamic stress on the bubble–particle aggregate is greater than the energy required for detachment. Schulze[35] found that the upper flotation size limit in the turbulent field is only a fraction of that in the quiescent field, which is supported by several experimental studies.[36–39] The detachment process is an overriding factor in the flotation of coarse particles in a turbulent field. An effective approach to improve coarse particle flotation is to minimize turbulence in flotation cells. From this point of view, the flotation column is much more favorable than the mechanical flotation cell for the flotation of coarse particles.

The probability of detachment (P_d) may be described by Eq. (17):

$$P_d = \frac{1}{1 + F_{at}/F_{de}} \tag{17}$$

where F_{at} represents the total attachment force and F_{de} the total detachment force. Equation (17) suggests that $P_d = 0.5$ when $F_a = F_d$; $P_d = 0$ when $F_a \gg F_d$; and $P_d = 1$ when $F_a \ll F_d$. Using Eqs. (11)–(13) and neglecting the drag force, one obtains:

$$\frac{F_{at}}{F_{de}} \approx \frac{3(1 - \cos\theta_d)\gamma}{g(\rho_p - \rho_w(1/2 + 3/4 \times \cos(\theta_d/2)))} \frac{1 + D_p/D_b}{D_p^2} \tag{18}$$

It can be readily seen from Eqs. (17) and (18) that F_{at}/F_{de} decreases and P_d increases with increasing D_p and increasing D_b. This conclusion is in agreement with the empirical correlation of Deglon et al.[40] that shows that the detachment rate constant for flotation increases with increasing D_b and D_p. Therefore, coarse particles are more likely to detach from air bubbles and use of small bubbles will increase flotation recovery of coarse particles.

It should be noted that most of the models discussed previously are based on a single bubble–single particle system, which does not represent the real

Marcel Dekker, Inc.
270 Madison Avenue, New York, New York 10016

flotation process where a swarm of bubbles is necessary. The prediction of particle–bubble interaction in a real system is complicated by the gas holdup effect, the interaction between neighboring bubbles, and the presence of multilayers of bubbles, all of which tend to straighten the liquid streamlines around a bubble and thus increase the overall probability of collection.

Flotation Kinetics

The first order flotation rate constant (k) is determined by:[6,40–44]

$$k = \frac{3V_g}{2D_b}P = \frac{1}{4}S_b P \tag{19}$$

$$P = P_c P_a (1 - P_d) \tag{20}$$

where V_g is the superficial gas rate, P is the probability of collection, and S_b is the bubble surface area flux. Since P_c, P_a, and P_d are all dependent on D_b and D_p, as discussed earlier, Eq. (19) indicates that k is strongly dependent on D_b and D_p. Finch and Dobby,[45] Heiskanen,[44] and Yoon[10] have shown that k varies as D_p^2/D_b^3 under quiescent conditions in flotation columns and approximately as $D_b^{-1.5}$ under well-mixed conditions in mechanical flotation cells. This relationship between k and D_b was obtained for fine particles under the assumption that $P_d = 0$. For coarse particles, smaller D_b should have more significant effects on k since P_d decreases with decreasing D_b. The previously discussion of individual processes in flotation indicates that the flotation recovery of particles can be enhanced effectively by use of smaller bubbles.

Levitation

After a particle is captured by a bubble and a stable particle–bubble aggregate is formed, levitation of the aggregate must follow to complete the flotation separation process. Small bubbles are favored to capture coarse particles, as discussed earlier; however, they may not have enough buoyancy to levitate the aggregate. It can be estimated that a bubble of 0.1 mm in diameter has a buoyancy to levitate particles of up to 0.069 mm with a density of 3.0 g/cm^3. The number of bubbles necessary to levitate a particle is a cubic function of D_p/D_b. Since large bubbles decrease the probabilities of collision and attachment and increase the probability of detachment, levitation of coarse particles can be strengthened by introduction of a certain number of large bubbles in addition to small bubbles and/or attachment of several small bubbles to the same particle. The most effective way of utilizing small bubbles

Marcel Dekker, Inc.
270 Madison Avenue, New York, New York 10016

for efficient capture and sufficient levitation of coarse particles is cavitation/gas nucleation. The fundamentals and mechanisms of this approach are discussed later.

Froth Phase Behavior

The behavior of the froth phase is another important aspect of flotation that affects flotation performance. Tao et al.[46] examined the effect of froth stability on column flotation and concluded that separation efficiency can be improved if froth stability is properly controlled. Tomlinson and Fleming[47] and Feteris et al.[48] showed that the flotation rate constant is directly proportional to the probability that a particle survives the cleaning action of the froth zone and reports to the froth product. Mineral particles have been reported to show pronounced effects on froth stability. However, controversy exists on whether particles stabilize or destabilize the froth. Szatkowski and Freyberger[49] observed that fine quartz particles rendered bubbles to be more resistant to coalescence and promoted the stable froth. Livshits and Dudenkov[50] believed that only coarse particles are able to act as buffers between bubbles and prevent bubble coalescence, consequently strengthening the stability of the froth. Klassen[51] reported that more hydrophobic particles had greater stabilizing effects on the froth. Johansson and Pugh[52] showed that particles of intermediate hydrophobicity (contact angle $\theta \approx 65^\circ$) would enhance froth stability but more hydrophobic particles ($\theta > 90^\circ$) would destabilize the froth, while more hydrophilic particles ($\theta < 40^\circ$) would not influence the froth properties. Moudgil et al.[12] suggested that coarse phosphate particles destabilize the froth. Tao et al.[46] concluded that particles could stabilize or destabilize the froth, depending on their size, surface hydrophobicity, and concentration.

Wiegel and Lawver[53] found that selectivity and recovery of coarse phosphate decrease as the height of the froth increases. Contini et al.[54] showed direct evidence that the transfer of particles from the collection zone to the froth zone in a flotation column decreases drastically with increasing particle size. Soto and Barbery[39] and Soto[55] reported that the absence of a froth phase improves coarse particle recovery and developed a very short column with only a 55-cm collection zone for coarse phosphate flotation. Soto[55] also found that use of negative bias (i.e., the tailings flow is smaller than the feed flow) in column flotation increases the flotation recovery of coarse particles. A negative bias reduces or even eliminates the froth layer, enhancing the probability of coarse particles reporting to the froth product. Oteyaka and Soto[8] developed a mathematical model for coarse particle flotation in columns with negative bias, and their simulation results indicate

that higher flotation recovery of coarse particles can be achieved by use of small bubbles and high air holdup.

PICOBUBBLE ENHANCED FLOTATION

Effect of Picobubbles on Particle Collision/Attachment

Tiny bubbles or gas nuclei of less than 1 μm and as large as 13.5 μm, referred to as picobubbles, naturally exist in liquids such as seawater and distilled water.[56,57] Picobubbles attach more readily to particles than large bubbles due to their lower ascending velocity and rebound velocity from the surface and higher surface free energy to be satisfied. More efficient attachment of particles and improved flotation rate have been observed when tiny bubbles co-exist with air bubbles commonly used in flotation cells.[58,59] Klassen and Mokrousov[51] showed that the combined flotation by gas nuclei from air supersaturation and by mechanically generated bubbles produced higher flotation recovery than by either of them alone. Gas nuclei or picobubbles on a particle surface activate flotation by promoting the attachment of larger bubbles (as shown in Fig. 3) since attachment between gas nuclei or picobubbles and large bubbles is more favored than bubble–solid attachment. In other words, picobubbles act as a secondary collector for particles, reducing flotation collector dosage, enhancing particle attachment probability, and

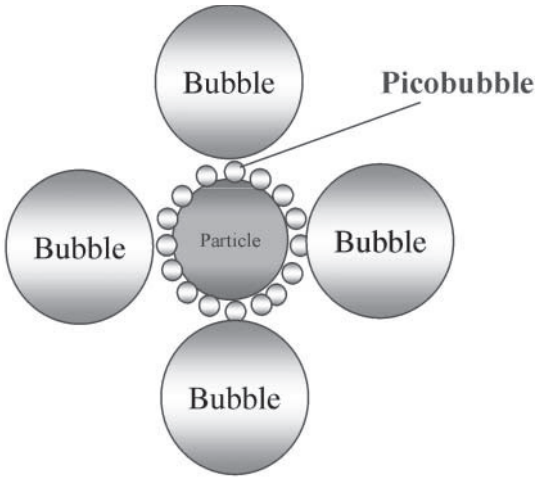

Figure 3. Enhanced bubble particle attachment by use of picobubbles.

MARCEL DEKKER, INC.
270 Madison Avenue, New York, New York 10016

reducing the detachment probability. This leads to substantially improved flotation recovery of poorly floating fine and coarse phosphate particles and reduced reagent cost, which is often the largest single operating cost in commercial mineral flotation plants. Application of this process to coal flotation resulted in an increase in flotation yield up to 15 wt%, a frother dose reduction of 10%, and a collector dose reduction of 90%.[60] Zhou et al.[61] showed that hydrodynamic cavitation significantly increased flotation kinetics of silica and zinc sulfide precipitates.

Hydrodynamic Cavitation

Hydrodynamic cavitation is the process of creation and growth of gas bubbles in a liquid due to the rupture of a liquid–liquid or a liquid–solid interface under the influence of external forces. The bubbles generated on a particle surface by cavitation naturally attach to the particle, eliminating the collision and attachment process, which is often the rate-determining step for flotation. Cavitation also improves the flotation efficiency of coarse particles by reducing the detachment probability during the rise of particle–bubble aggregate in liquid. This is best illustrated in Fig. 4 where the large bubble represents the one produced by breaking the external air and smaller ones (picobubbles) are created by cavitation. While the large bubble may run away

Figure 4. Reduced detachment probability by picobubbles.

from the particle, the cavitation bubbles, particularly those underneath the particle, will push the particle upward, facilitating particle recovery.

Without cavitation-generated bubbles, particles will detach from the bubble surface when the capillary force and other attachment forces are exceeded by detachment forces, such as the viscous or drag force (F_d), the gravitational force, and the hydrostatic pressure. It should be noted that the drag force is velocity dependent, as shown in Eqs. (21) and (22):

$$F_d = 3\pi D_p \eta u \quad \text{(laminar condition)} \tag{21}$$

$$F_d = \frac{C_d \pi}{8} \rho D_p^2 u^2 \quad \text{(turbulent condition)} \tag{22}$$

where D_p is the particle diameter, η is the dynamic viscosity of fluid, u is the particle rising velocity, ρ is the fluid density, and C_d is the drag coefficient, which depends on the Reynolds number.

The drag force increases as the bubble–particle aggregate rises in the flotation cell. If the cell is deep, the particle is likely to detach from the bubble surface when the rising velocity reaches a certain value. Equations (21) and (22) also indicate that the drag force is directly proportional to the particle diameter; coarse particles are more likely to detach from the bubble surface than fine particles. This is the main reason for low flotation recovery of coarse particles, which is recognized by Soto and Barbery,[39] Ralston et al.,[31,32] and Ralston and Dukhin.[9] Thus, a shallow flotation cell is essential for coarse particle flotation, which is confirmed by industrial practices.[11,39]

Cavitation takes place in the form of gas supersaturation or hydrodynamic cavitation. Tiny bubbles may form by gas supersaturation in liquid from preexisting gas nuclei trapped in crevices of solid particles.[62,63] Solid particles with rough and hydrophobic surfaces are known to promote bubble formation in liquid.[64,65] Hydrodynamic cavitation occurs when the pressure at a point in a liquid is momentarily reduced below its vapor pressure due to high flow velocity.[66] Minute air or vapor-filled bubbles are carried on by the flow to regions of higher pressure. Hydrodynamic cavitation is well described by Bernoulli's equation:

$$P + \frac{1}{2}\rho U^2 = C \text{ (constant)} \tag{23}$$

in which U is the water flow velocity at a point where the pressure is P, ρ is the liquid density. Rearranging Eq. (23) yields:

$$U^2 + \frac{2P}{\rho} = \frac{2C}{\rho} \tag{24}$$

MARCEL DEKKER, INC.
270 Madison Avenue, New York, New York 10016

which indicates that the pressure will be negative when the water flow velocity U exceeds $\sqrt{2C/\rho}$.

The venturi tube shown in Fig. 5 is the most widely used hydrodynamic cavitation device. Liquid flow accelerates in the conical convergent zone due to the narrowing diameter. The liquid in the cylindrical throat is higher in flow velocity and lower in pressure than liquid in the entrance cylinder, resulting in cavitation. The differential pressure between the entrance cylinder and the cylindrical throat measured by the manometers is indicative of cavitation behavior. The presence of tiny pockets of undissolved gas in crevices on mineral particles assists the cavitation as a result of the expansion of these gas pockets under the negative pressure. Holl[67] found that the cavitation was directly proportional to the dissolved air content in liquid. Addition of organic chemicals such as frothers produces smaller and more copious cavities by stabilizing the cavity and preventing cavity collapse and coalescence.

CONCLUSIONS

Based on the above discussion, the following conclusions can be drawn:

1. The low flotation recovery of fine particles is mainly caused by the low probability of bubble–particle collision; the main reason for poor flotation recovery of coarse particles is the high probability of detachment of particles from the bubble surface.
2. Use of small bubbles increases the probability of collision and adhesion and reduces the probability of detachment.

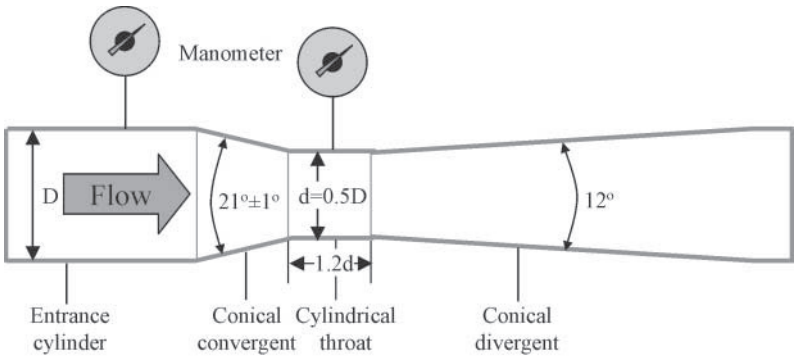

Figure 5. Venturi cavitation tube and major parameters.

3. Larger bubbles are needed to provide sufficient levitation of coarse particle–bubble aggregate.
4. Increased surface hydrophobicity promotes recovery of coarse mineral particles by reducing the probability of detachment.
5. Use of a shorter flotation column minimizes bubble growth, which in turn reduces viscous force and increases the excess force.
6. Reduction of turbulence in the flotation cell creates more favorable hydrodynamic conditions for coarse particles.
7. Elimination of froth phase for enhanced flotation recovery of coarse particles.
8. Negative bias in column flotation should be used for coarse particles to facilitate ascending of bubble particle aggregates and positive bias for fine particles to reduce nonselective hydraulic entrainment.

REFERENCES

1. Gaudin, A.; Grob, J.; Henderson, H. *Effect of Particle Size on Flotation*; Technical Publication No. 414, AIME, 1931.
2. Morris, T.M. Measurement and evaluation of the rate of flotation as a function of particle size. Min. Eng-Littleton **1952**, *4* (8), 794–798.
3. Trahar, W.J.; Warren, L.J. The floatability of very fine particles—a review. Inter. J. Miner. Process. **1976**, *3*, 103–131.
4. King, R.P. Flotation of fine particles. In *Principles of Flotation*; King, R.P., Ed.; South African Institute of Mining and Metallurgy: Johannesburg, 1982.
5. Feng, D.; Aldrich. Effect of particle size on flotation performance of complex sulfide ores. Miner. Eng. **1999**, *12* (7), 721–731.
6. Yoon, R.-H.; Luttrell, G.G.; Adel, G.T.; Mankosa, M.J. Recent advances in fine coal flotation. In *Advances in Coal and Mineral Processing Using Flotation*; Chander, S., Ed.; Society of Mining Engineers: Littleton, CO, 1989; Chap. 23, 211–218.
7. Drzymala, J. Characterization of materials by Hallimond tube flotation. Part 2: maximum size of floating particles and contact angle. Int. J. Miner. Process. **1994**, *42*, 153–167.
8. Oteyaka, B.; Soto, H. Modelling of negative bias column for coarse particles flotation. Miner. Eng. **1995**, *8* (1/2), 91–100.
9. Ralston, J.; Dukhin, S.S. The interaction between particles and bubbles. Colloid. Surface. **1999**, *151*, 3–14.
10. Yoon, R.-H. The role of hydrodynamic and surface forces in bubble-particle interaction. Inter. J. Miner. Proces. **2000**, *58*, 128–143.

Marcel Dekker, Inc.
270 Madison Avenue, New York, New York 10016

11. Van Der Spuy, R.C.M.; Ross, V.E. The recovery of coarse minerals by agglomeration and flotation. Miner. Eng. **1991**, *4* (7–11), 1153–1166.
12. Moudgil, B.M. *Enhanced Recovery of Coarse Particles During Phosphate Flotation*; Final Report to Florida Institute of Phosphate Research, 1992; Publication Number 02-067-099.
13. Maksimov, I.I.; Otrozhdennova, L.A.; Borkin, A.D.; Yemelyanov, M.F.; Koltunova, T.Y.; Malinovskaya, N.D.; Nechay, L.A. An investigation to increase the efficiency of coarse and fine particle flotation in ore processing of non-ferrous metals. Proceedings of XVIII International Mineral Processing Congress, 1993; 685–687.
14. El-Shall, H. *Bubble Generation, Design, Modeling and Optimization of Novel Flotation Columns for Phosphate Beneficiation*; Final Report to Florida Institute of Phosphate Research, FIPR: 1999.
15. Kohmuench, J.; Luttrell, G.H.; Mankosa, M. Testing of the hydrofloat separator for recovery of coarse phosphate. In *Beneficiation of Phosphates, Advances in Research and Practice*; Zhang, P., Elshall, H., Wiegel, R., Eds.; SME Inc.: Littleton, CO, 1999; 215–226.
16. Kohmuench, J.; Mankosa, M.; Shoniker, J. Upgrading coarse phosphate sands using the hydrofloat separator. In *Beneficiation of Phosphates III*, St. Pete Beach, FL, December 2–7, 2001.
17. El-Shall, H.; Sharma, R.; Abdel-Khalek, N.A.; Svoronos, S.; Gupta, S. Column flotation of Florida phosphate: an optimization study. Miner. Metall. Proc. **2001**, *18* (3), 142–146.
18. Weber, M.E. Collision efficiencies for small particles with a spherical collector at intermediate Reynolds numbers. Sep. Processes Technol. **1981**, *2*, 29–33.
19. Weber, M.E.; Paddock, D. Interceptional and gravitational collision efficiencies for single collectors at intermediate Reynolds numbers. J. Colloid Interface Sci. **1983**, *94*, 328–335.
20. Yoon, R.-H.; Luttrell, G.H. The effect of bubble size on fine particle flotation. Miner. Process. Extr. Metall. Rev. **1989**, *5*, 101–122.
21. Schubert, H.; Bischofberger, C. On the optimization of hydrodynamics in flotation processes. *Proceedings of 13th Int. Miner. Process. Cong.*, Warszawa, 1979; 2, 1261–1287.
22. Sutherland, K.L. Physical chemistry of flotation: XI. Kinetics of the flotation process. J. Phys. Chem. **1949**, *52*, 394–425.
23. Gaudin, A.M. *Flotation*, 2nd Ed.; McGraw-Hill: New York, 1957.
24. Schulze, H.J. Hydrodynamics of bubble-mineral particle collisions. Min. Process. Extractive Metall. Rev. **1989**, *5*, 43–76.
25. Dai, Z.; Dukhin, S.S.; Fornasiero, D.; Ralston, J. The inertial hydrodynamic interaction of particles and rising bubbles with mobile surfaces. J. Colloid Interface Sci. **1998**, *197*, 275–292.

MARCEL DEKKER, INC.
270 Madison Avenue, New York, New York 10016

26. Langmuir, I.; Blodgett, K. Mathematical investigation of water droplet trajectories. Gen. Elec. Comp. Rep. **1945**.
27. Langmuir, I.; Blodgett, K. Mathematical investigation of water droplet trajectories. J. Meteorol. **1948**, *5*, 175–181.
28. Dai, Z.; Fornasiero, D.; Ralston, J. Particle-bubble collision models—a review. Adv. Colloid Interfac. **2000**, *85*, 231–256.
29. Luttrell, G.H.; Yoon, R.-H. A hydrodynamic model for bubble-particle attachment. J. Colloid Interface Sci. **1992**, *154*, 129–137.
30. Mao, L.; Yoon, R.-H. Predicting flotation rates using a rate equation derived from first principles. Int. J. Miner. Process. **1997**, *51*, 171–181.
31. Ralston, J.; Dukhin, S.S.; Mischuk, N.H. Bubble-particle attachment and detachment in flotation. Int. J. Miner. Process. **1999a**, *56*, 133–164.
32. Ralston, J.; Dukhin, S.S.; Mischuk, N.H. Inertial hydrodynamic particle-bubble interaction in flotation. Int. J. Miner. Process. **1999b**, *56*, 207–256.
33. Kirchberg, H.; Topfer, E. The mineralization of air bubbles in flotation. In *Proc. VII Min. Process. Congress*; Gordon and Breach: New York, 1965; 157–168.
34. Cheng, T.; Holtham, P.N. The particle detachment process in flotation. Miner. Eng. **1995**, *8* (8), 883–891.
35. Schulze, H.J. *Physico-Chemical Elementary Processes in Flotation*; Elsevier; 1984.
36. Sun, S.; Zimmerman, R.E. The mechanism of coarse coal and mineral froth flotation. Min. Eng-Littleton **1950**, *187* (5), 616–620.
37. Arbiter, N.; Steinenger, J. Hydrodynamics of flotation machine. In *Mineral Processing*; Pergamon, 1965; 595.
38. Bensley, C.N.; Nicol, S.K. The effect of mechanical variables on the flotation of coarse coal. Coal Preparation **1985**, *1*, 189–205.
39. Soto, H.S.; Barbery, G. Flotation of coarse particles in a counter-current column cell. Miner. Metall. Proc. **1991**, *8* (1), 16–21.
40. Deglon, D.A.; Sawyerr, F.; O'Connor, C.T. A model to relate the flotation rate constant and the bubble surface area flux in mechanical flotation cells. Mineral Engineering **1999**, *12* (6), 599–608.
41. Gorain, B.K.; Franzidis, J.P.; Manlapig, E.V. Studies on impeller type, impeller speed and air flow rate in an industrial scale flotation cell. Part 1. Effect of bubble size distribution. Miner. Eng. **1995**, *8* (6), 615–635.
42. Yoon, R.-H.; Mao, L. Application of extended DLVO theory: IV. Derivation of flotation rate equation from first principles. J. Colloids Interface Sci. **1996**, *181*, 613–626.
43. Gorain, B.K.; Franzidis, J.P.; Manlapig, E.V. Studies on impeller type, impeller speed and air flow rate in an industrial scale flotation cell. Part 4. Effect of bubble surface area flux on floattion performance. Miner. Eng. **1997**, *10* (4), 367–379.

Marcel Dekker, Inc.
270 Madison Avenue, New York, New York 10016

44. Heiskanen, K. On the relationships between flotation rate and bubble surface area flux. Miner. Eng. **2000**, *13* (2), 141–149.
45. Finch, J.A.; Dobby, G.S. *Column Flotation*; Pergamon: Oxford, 1990; 180.
46. Tao, D.; Luttrell, G.H.; Yoon, R.-H. A parametric study of froth stability and its effect on column flotation of fine particles. Inter. J. Miner. Process. **2000**, *59*, 25–43.
47. Tomlinson, H.S.; Fleming, M.G. Flotation rate studies. Proceedings, 6th Inter. Min. Proc. Congress, Cannes, Pergamon: Oxford, 1965; 563–579.
48. Feteris, S.M.; Frew, J.A.; Jowett, A. Modelling the effect of froth depth in flotation. Inter. J. Miner. Process. **1987**, *20*, 121–135.
49. Szatkowski, M.; Freyburger, W.L. Kinetics of flotation with fine bubbles. Trans. Inst. Min. Metall. Sec. C **1985**, *94*, C61–70.
50. Livshits, A.K.; Dudenkov, S.V. Some factors in flotation froth stability. In *Proc. of VIIth Int. Proc.*; Longr Gordon and Breach: New York, NY, 1965; 597–621.
51. Klassen, V.I.; Mokrousov, V.A. *An Introduction to the Theory of Flotation*; Butterworth: London, 1963.
52. Johansson, G.; Pugh, R.J. The influence of particle size and hydrophobicity on the stability of mineralized froths. Inter. J. Miner. Process. **1992**, *34*, 1–21.
53. Wiegel, R.L.; Lawver, J.E. Reducing theory to practice (or vice versa) in mineral processing. In *Advances in Mineral Processing*; SME/AIME; 1986; 685–694.
54. Contini, N.J.; Wilson, N.S.; Dobby, G. Measurements of rate data in flotation columns. Column Flotation '88, SME/AIME; 1988; 69–80.
55. Soto, H.S. *Development of Novel Flotation Elutriation Method for Coarse Phosphate Beneficiation*; Final Report to Florida Institute of Phosphate Research, 1992; Publication Number 02-070-098.
56. Johnson, B.D.; Cooke, R.C. Generation of stabilized microbubbles in seawater. Science **1981**, *213*, 209–211.
57. Yount, D.E. Growth of bubbles from nuclei. *Supersaturation and Bubble Formation in Fluids and Organisms. An International Symposium*; Brubakk, A.O., Hemmingsen, B.B., Sundnes, G., Eds.; The Royal Norwegian Society of Sciences and Letters, The Foundation: Trondheim, Norway, 1989.
58. Dziensiewicz, J.; Pryor, E.J. An investigation into the action of air in froth flotation. Trans. IMM., London **1950**, *59*, 455–491.
59. Shimoiizaka, J.; Matsuoka, I. Applicability of air-dissolved flotation for separation. *Proc. XIV International Mineral Processing Congress*; Toronto, Canada, Oct. 17–23, 1982.

60. Attalla, M.; Chao, C.; Nicol, S.K. The role of cavitation in coal flotation. *Proceedings of the Eigth Australian Coal Preparation Conference*; Port Stephens, Nov 12–16, 2000; 337–250.
61. Zhou, Z.A.; Xu, Z.; Finch, J.A.; Hu, H.; Rao, S.R. Role of hydrodynamic cavitation in fine particle flotation. Int. J. Miner. Process. **1997**, *51*, 139–149.
62. Finkelstein, Y.; Tamir, A. Formation of gas bubbles in supersaturated solutions of gases in water. AIChE J. **1985**, *31*, 1409–1419.
63. Flynn, H.G. Physics of acoustic cavitation in liquids. In *Physical Acoustics, Principles and Methods*; Mason, W.P., Ed.; Academic Press: New York, 1964; Vol. 1–Part B, 57–172.
64. Ryan, W.L.; Hemmingsen, E.A. Bubble formation in water at smooth hydrophobic surfaces. J. Colloid. Interface Sci. **1993**, *157*, 312–317.
65. Gerth, W.A.; Hemmingsen, E.A. Heterogeneous nucleation of bubbles at solid surfaces in gas-supersaturated solutions. J. Colloid. Interface Sci. **1980**, *74*, 80–89.
66. Young, F.R. *Cavitation*; McGraw-Hill Book Company: London, 1989.
67. Holl, J.W. Nuclei and cavitation. J. Basic Engineering **1970**, *92*, 681–688.

Received June 2003
Revised September 2003